

A Combined ONIOM Quantum Chemical–Molecular Dynamics Study of Zinc–Uracil Bond Breaking in Yeast Cytosine Deaminase

Lishan Yao,^{†,§} Honggao Yan,^{*,†,§} and Robert I. Cukier^{*,†,§}

Department of Chemistry, Department of Biochemistry and Molecular Biology, and MSU Center for Biological Modeling, Michigan State University, East Lansing, Michigan 48824

Received: July 8, 2006; In Final Form: October 17, 2006

A QM/MM method that combines ONIOM quantum chemistry and molecular dynamics is developed and applied to a step in the deamination of cytosine to uracil in yeast cytosine deaminase (yCD). A two-layer ONIOM calculation is used for the reaction complex, with an inner part treated at a high level for the chemical reaction (bond breaking) and a middle part treated at a lower level for relevant protein residues that are frozen in the quantum optimization. An outer layer (protein and solvent) is treated using MD. Configurations for the entire system are generated using MD and optimized with ONIOM. The method permits the use of high-level quantum calculations along with sufficient configurational sampling to approximate the potential of mean force for certain bond-breaking reactions. A previously proposed reaction mechanism for deamination (Sklenak, S.; Yao, L. S.; Cukier, R. I.; Yan, H. G. *J. Am. Chem. Soc.* **2004**, *126*, 14879) requires breaking the bond between a catalytic zinc and the O4 of uracil in order to permit product release. Using an ONIOM approach, direct bond cleavage was found to be energetically unfavorable. In the work presented here, the combined ONIOM MD method is used to show that the barrier for bond cleavage is small, ~ 3 kcal/mol, and, consequently, should not be the rate-limiting step in the reaction.

1. Introduction

Yeast cytosine deaminase (yCD) catalyzes the deamination of cytosine to uracil (Figure 1a) as well as 5-fluorocytosine (5-FC) to the anticancer drug 5-fluorouracil (5-FU). It has been observed that product release is the rate-limiting step during the activation of 5-FC,¹ and presumably the same holds for the enzymatic deamination of the normal substrate, cytosine. One reason for this slow product release might be the formation of a Zn–O4 bond between the protein and product, 5-FU, as shown for uracil in Figure 1b. In our previous work,² the mechanistic steps to convert cytosine to the Zn–O4 intermediate were studied by quantum chemical methods. The cytosine deamination proceeds via a sequential mechanism involving the protonation of the N3 of cytosine, a nucleophilic attack on C4 by the Zn-coordinated hydroxide, and the cleavage of the C4–N4 bond. Once the Zn–O4 intermediate is formed, our calculations² showed that direct Zn–O4 bond cleavage is nearly impossible based on two-layer ONIOM (B3LYP/PM3) quantum chemical calculations.^{3–6} As an alternative, an oxygen exchange mechanism was proposed to assist this bond breaking, which gave the highest barrier, ~ 9 kcal/mol, for the activation energy of the whole reaction cycle. However, our recent experiments (unpublished data) show that, although this oxygen exchange does occur, it is so slow that it is unlikely to be the mechanism for cleavage of the Zn–O4 bond.

In this previous two-layer ONIOM study, a fraction of the protein was selected (residues around the active site), and atoms

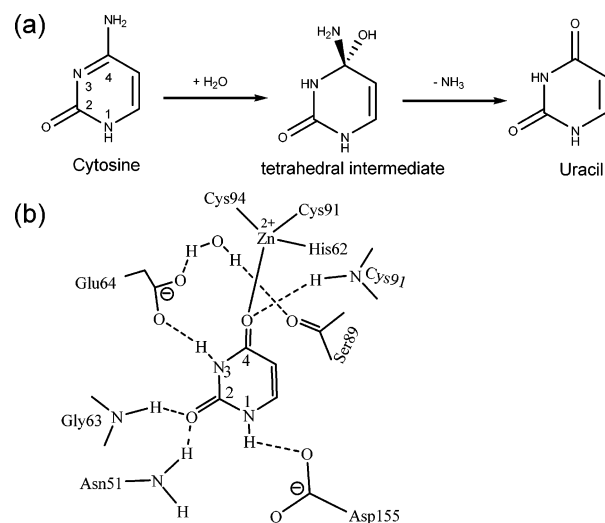


Figure 1. (a) The deamination of cytosine catalyzed by yCD. (b) Zn–O4–uracil intermediate along with several key residues that form part of the inner and middle layers for the ONIOM calculation. Hydrogen bonds are indicated by dashed lines.

in the outer layer were fixed to prevent them from moving away unrealistically, while atoms in the inner layer were optimized. If the rearrangement of the active site is rather small during the catalysis, this protocol works well, but when the rearrangement is significant, some atoms in the outer layer have to move to accommodate this change. Then, freezing the outer layer will give unrealistic results.

The above experimental and computational results motivate a reinvestigation of the mechanism of Zn–O4 bond breaking. In particular, it is clear that the dynamics of the whole protein, or at least the residues around the active site, have to be incorporated into the calculation. QM/MM simulation methods

* To whom correspondence may be addressed. Professor Robert I. Cukier. E-mail: cukier@cem.msu.edu. Phone: 517-355-9715 x 263. Fax: 517-353-1793. Professor Honggao Yan. E-mail: yanh@msu.edu. Phone: 517-353-5282. Fax 517-353-9334.

[†] Department of Chemistry.

[‡] Department of Biochemistry and Molecular Biology.

[§] MSU Center for Biological Modeling.

have to be used to fully describe this process. The challenge is that, in order to model complexes containing Zn ions, reliable QM methods should be used,^{2,7} which would be very costly if used in combination with a MD simulation. For example, one single-point ONIOM (B3LYP/PM3) calculation of the yCD system that we carried out² takes ~80 min in a two-processor Linux workstation with 2.1 GHz CPU speed. With the 2 fs MD time step, a 1 ns QM/MM simulation would take years. Accurate statistical mechanical sampling with a high-level QM method for this system is certainly not feasible.

A number of QM/MM protocols have been developed to incorporate configurational sampling while accounting for chemical transformations, which involve a tradeoff between the quality (cost) of the quantum chemical part and the extent of configurational sampling.^{8–23} Some of these approaches use semiempirical methods to reduce the quantum part cost and permit more configurational sampling, while others use higher-level quantum methods at the expense of sampling. The ONIOM method,^{3–6} with its separation of a system into layers, with higher-level methods used for inner and lower-level methods used for outer layers, is an attempt to reduce the cost of calculation while retaining accuracy of predictions, but it does not incorporate the effect of different configurations. Thus, many ONIOM calculations of enzymatic systems are performed for static structures either taken from X-ray structures^{24–26} or averaged MD snapshots,^{27,28} and the enzyme is usually truncated to only include important regions such as the active site. Methods are being developed that can permit the use of high-level quantum methods yet permit adequate sampling. For example, Yang and his colleagues developed a minimum-energy-path method where the QM region is optimized along the reaction coordinate(s) and frozen during simulations.²⁹ The free-energy change of the QM region is calculated based on the energy change and the entropy change, as calculated by harmonic frequency analysis. The free-energy change of the MM region is calculated by using a free-energy perturbation method.

In this paper, we propose a protocol that incorporates the dynamics of both the QM and MM regions and permits calculation of the potential of mean force along a reaction coordinate. It combines conventional MD and ONIOM procedures in an approximate manner that permits the use of high-level methods and reasonably extensive MD sampling. The method is used to obtain the barrier for the Zn–O4 bond cleavage step necessary for product release in yCD.

2. Methodology

A. Two-Step Method Combining MD and ONIOM. The system of interest consists of a protein, its bound ligand, and explicit waters of solvation. Our strategy is to treat the ligand and catalytically important residues with a high-level QM method (core layer), the surrounding residues in the active site with a low-level QM method (middle layer), and the rest of the protein, including water, with molecular mechanics (outer layer).

With the Born–Oppenheimer approximation and assuming the electronic degrees of freedom have been integrated out, the Hamiltonian of the whole system is

$$H_{\text{tot}} = H_{\text{h}}^{\text{q}} + H_{\text{l}}^{\text{q}} + H_{\text{hl}}^{\text{q}} + H_{\text{r}}^{\text{m}} + H_{\text{hr}}^{\text{qm}} + H_{\text{lr}}^{\text{qm}} \quad (2.1)$$

where superscript q (m) means the term is treated with quantum mechanics (classical mechanics) and where h, l, and r denote high level (quantum), low level (quantum), and the rest (molecular mechanics), respectively.

For a system with N particles, the canonical ensemble distribution function is

$$\rho(\mathbf{p}^{3N}, \mathbf{r}^{3N}) = \frac{\exp(-\beta H_{\text{tot}}(\mathbf{p}^{3N}, \mathbf{r}^{3N}))}{\int \exp(-\beta H_{\text{tot}}(\mathbf{p}^{3N}, \mathbf{r}^{3N})) d\mathbf{p}^{3N} d\mathbf{r}^{3N}} \quad (2.2)$$

where \mathbf{p}^{3N} and \mathbf{r}^{3N} are vectors defining Cartesian momenta and coordinates of the whole system and where β is $1/kT$ in which k is Boltzmann constant and T is temperature in kelvin. If we are interested in a chemical process in the core layer, we need to define a specific reaction coordinate ξ (e.g., distance between two atoms in a bond cleavage). A coordinate transformation needs to be introduced from Cartesian coordinates to a set of generalized coordinates that contains $\xi, \mathbf{r}^{3N} \rightarrow (\mathbf{q}^{3N-1}, \xi)$. In addition, a corresponding transformation is made on the conjugate momentum according to $\mathbf{p}^{3N} \rightarrow (\mathbf{p}_{\text{q}}^{3N-1}, \mathbf{p}_{\xi})$ so that $d\mathbf{p}^{3N} d\mathbf{r}^{3N} = d\mathbf{p}_{\text{q}}^{3N-1} d\mathbf{q}^{3N-1} d\mathbf{p}_{\xi} d\xi$. Thus, the potential of mean force is

$$\begin{aligned} \text{PMF}(R) &= -\frac{1}{\beta} \ln \frac{\int \exp(-\beta H_{\text{tot}}(\mathbf{p}^{3N}, \mathbf{r}^{3N})) \delta(\xi - R) d\mathbf{p}^{3N} d\mathbf{r}^{3N}}{\int \exp(-\beta H_{\text{tot}}(\mathbf{p}_{\text{q}}^{3N-1}, \mathbf{q}^{3N-1}, \mathbf{p}_{\xi}, \xi)) \delta(\xi - R) d\mathbf{p}_{\text{q}}^{3N-1} d\mathbf{q}^{3N-1} d\mathbf{p}_{\xi} d\xi} \\ &= -\frac{1}{\beta} \ln \frac{Q}{Q} \end{aligned} \quad (2.3)$$

where $Q = \int \exp(-\beta H_{\text{tot}}(\mathbf{p}^{3N}, \mathbf{r}^{3N})) d\mathbf{p}^{3N} d\mathbf{r}^{3N}$ is the partition function, and the delta function maintains the reaction coordinate ξ at value R .

The mean force is given by

$$-\frac{\partial \text{PMF}(R)}{\partial R} = -\left\langle \frac{\partial H_{\text{tot}}}{\partial \xi} \right\rangle_{\xi=R} \quad (2.4)$$

where $\langle \dots \rangle_{\xi=R}$ denotes a conditional ensemble average. Since ξ is only a function of the coordinates of certain atoms in the high-level QM part, eq 2.4 can be approximated as

$$\frac{\partial \text{PMF}(R)}{\partial R} = \left\langle \frac{\partial (H_{\text{h}}^{\text{q}} + H_{\text{hl}}^{\text{q}} + H_{\text{hr}}^{\text{qm}})}{\partial \xi} \right\rangle_{\xi=R} \approx \left\langle \frac{\partial (H_{\text{h}}^{\text{q}} + H_{\text{hl}}^{\text{q}})}{\partial \xi} \right\rangle_{\xi=R} \quad (2.5)$$

provided that the interaction between the core and outer layer is very small. The outer layer does influence the mean force through the ensemble average. To estimate this average, a certain number of MD snapshots need to be generated with the constraint that $\xi = R$. Then, the potential of mean force can be evaluated from eq 2.5 by integration.

$$\begin{aligned} \text{PMF}(R_1) - \text{PMF}(R_0) &= \int_{R_0}^{R_1} \frac{\partial \text{PMF}(R)}{\partial R} dR = \\ &= \int_{R_0}^{R_1} \left\langle \frac{\partial (H_{\text{h}}^{\text{q}} + H_{\text{hl}}^{\text{q}})}{\partial \xi} \right\rangle_{\xi=R} dR \end{aligned} \quad (2.6)$$

As discussed above, this QM/MM simulation is impractical with current computer resources due to the expensive QM calculation. Approximations have to be introduced to evaluate the mean force more efficiently, and we propose the following two-step method. First, in step 1, a MD simulation with all of the atoms treated classically is performed, with the restraint that $\xi = R$. Second, in step 2, a certain number of snapshots are chosen for a two-layer ONIOM optimization, with the high- and low-level

QM method the same as would be used in an “ideal” QM/MM simulation. In the ONIOM optimization, the low-level layer is fixed, and the high-level layer is fully optimized with the constraint, $\xi = R$. Then, the force between two atoms can be calculated and averaged over the snapshots by using eq 2.5. By repeating the two steps with different constraint distances, the PMF can be calculated with the use of eq 2.6. Since the chemical bond cleavage process cannot be described by the MM method, the core layer has to be optimized using a high-level QM method before the force calculation, which acts as a refinement of the core structure. The presence of the outer layer in step 1 incorporates the effect of the rest of the protein and the (explicit) solvent on the core and middle layer. It should provide reasonable configurations for the middle layer as a function of the current reaction coordinate value and will also keep the middle layer from “evaporating”.

The main errors introduced by this approximation method come from the core and middle layers in the MD simulation of step 1. The first error comes from the MM treatment of the core layer. The classical treatment of the core in the simulation may not be able to generate good conformations for the force calculation. Thus, the ONIOM optimization has to be performed in step 2. For the middle layer, the use of MM in the MD simulation might also introduce an error. However, since there is no chemical reaction occurring in the middle layer, MM should be a reasonable approximation to a low-level QM method to describe the configuration of the protein. If the MM of the middle layer responds properly to the restrained changes in the core layer and generates corresponding conformational changes, then the ONIOM optimization in step 2 will produce an accurate core region conformation, which will give a good estimate of the force. There are also errors due to the lack of a polarization response of the outer MM layer to changes in the core and the middle layer. These should be small, as the core region with its changing charge distribution along the reaction coordinate is protected from the outer layer by the middle layer.

To guarantee that these errors are small, two conditions have to be fulfilled. First, that MM is a good method to describe the initial state, which is likely to be true with current force fields because the initial state is a well-defined state obtained from a crystal structure. Second, during the reaction process, the modification of the core is small, and, consequently the quantum effect changes to the middle layer are small compared to the MM changes produced by the electrostatic and van der Waals interactions. In summary, the PMF quality will depend primarily on the quality of the MM treatment of the core system and the complexity of the reaction process in this two-step protocol.

B. MD Simulation and ONIOM Calculation of the yCD–Uracil Complex. A 2 ns MD simulation was previously performed for the yCD–uracil complex at constant temperature (300 K) and at constant volume.³⁰ The details of the MD simulation protocol are provided therein, and we use the same protocol here. MD charges of the complex formed from Zn, its three ligated residues, His62, Cys91, Cys94, as well as Asp155 (all atoms), and one water molecule (coordinated with the Zn) were derived by using the AMBER antechamber program (RESP methodology).^{30,31} In that simulation, the active site Zn and uracil O4 were linked by a harmonic potential with the force constant of 300 kcal/mol Å² and the equilibrium distance of 1.97 Å. In order to see what happens after the Zn–O4 bond breaks, a 1 ns MD simulation was carried out starting from one snapshot of the preceding simulation with the harmonic potential removed. During this simulation, the Zn–O4 distance increased to ~3.6 Å. One MD snapshot was selected with the Zn–O4

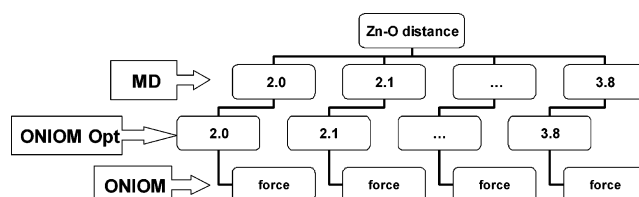


Figure 2. A flow chart of the MD–ONIOM combination used in the Zn–O bond cleavage study.

distance of 3.86 Å and trimmed for a two-layer ONIOM (B3LYP/PM3) optimization using Gaussian 03³² with the same setup as in the previous² study. The middle layer (outer layer in the ONIOM calculation) is fixed and treated by PM3, including residues Ile33, Asn51, Thr60, Leu61, Gly63, Ile65, Leu88, Ser89, Pro90, Asp92, Met93, Thr95, Phe114, Trp152, Phe153, Glu154, Asp155, and Ile156. The core layer (inner layer in the ONIOM calculation) is fully optimized by using the B3LYP³³ functional and the 6-31G** basis set that, as found previously,² leads to excellent agreement with the geometry obtained from the X-ray structure.³⁴ It includes uracil, Glu64, Zn, and the Zn-coordinated residues, His62, Cys91, and Cys94. Glu64 is included in the inner layer, as its key role in the deamination reaction has been established in the closely related enzyme, cytidine deaminase.^{35,36} The resulting ONIOM-optimized Zn–O4 distance is similar to that obtained from the MD simulation. This distance was scanned from 3.8 to 2.0 Å, with the core region optimized at each distance to obtain the energy changes along the Zn–O4 bond cleavage reaction coordinate. Another static structure of the uracil complex from the previous ONIOM calculation² with a Zn–O4 distance of 2.06 Å was generated from the yCD X-ray structure of the inhibitor (2-pyrimidinone) complex. Then, the Zn–O4 distance was scanned to compare the energy profile to that generated from the MD snapshot. Since, in the ONIOM calculations, the middle layer is fixed, if the change of the middle layer is very small during Zn–O4 bond cleavage, then, in reality, these two energy profiles should be very similar. In other words, if the profiles are quite different, then the middle layer must have changed significantly.

A 1 ns MD simulation was performed with a harmonic potential between Zn–O4 maintained but with the equilibrium distance changed by 0.1 Å every 50 ps from 2.0 to 3.8 Å, starting from one MD snapshot of the first simulation. The force constant of the harmonic potential is 300 kcal/mol. The coordinates were saved every 2 ps, and the first 20 ps were used as the equilibration period. For each Zn–O distance, five snapshots were chosen evenly in time and optimized by the ONIOM method, as described above. Then, the force on O4 from all of the other atoms, projected along the Zn–O4 vector, was calculated and averaged over five snapshots. The two-step process is outlined in Figure 2. The error of the force average is rather small, based on its standard deviation (see the Results and Discussion section), except at a distance of 2.3 Å, where 10 snapshots were used in the ONIOM calculation.

3. Results and Discussion

A. Scan with the Outer Layer Fixed. After Glu64 transfers two protons from the Zn-bound water molecule to cytosine, ammonia is formed and released, but the O4 of uracil is still covalently bound to the Zn atom.² In our previous calculations,² it appeared that direct Zn–O4 bond cleavage is extremely difficult, but one potential problem of that calculation was that the outer layer of the protein was fixed at the crystal structure

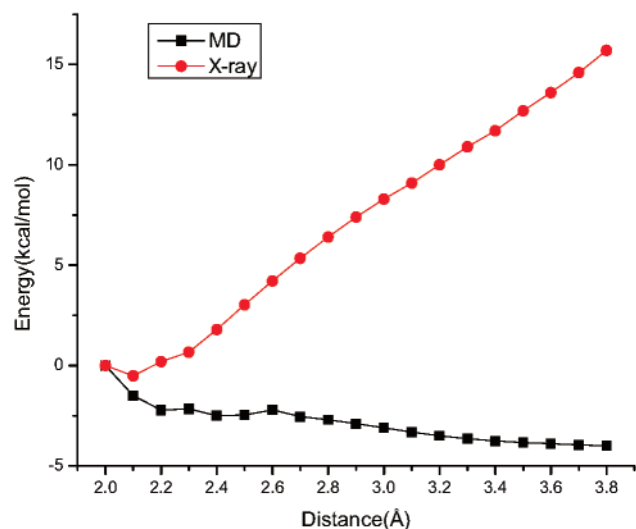


Figure 3. ONIOM energy changes along the Zn–O4 distance scan. The red (X-ray) line corresponds to the outer layer fixed at the X-ray coordinates. The black (MD) line corresponds to a relaxed configuration obtained from a MD simulation snapshot.

coordinates. If some of these residues need to rearrange themselves during breakage of the Zn–O4 bond, fixing the outer layer will make the reaction coordinate barrier artificially high due to steric clashes. The ONIOM optimizations were carried out to scan the Zn–O4 distance from 2.0 to 3.8 Å, based on the Zn–O4-bound product complex structure generated from the yCD inhibitor crystal structure.^{2,34,37} A 1 ns MD simulation (see the Methodology section) was performed with the bond restraint between Zn and O4 removed, which effectively gives a relaxed system with the Zn–O4 bond broken. Then, the same ONIOM optimizations were performed based on the final MD snapshot. By comparing these two energy profiles, we can see whether the constraint of the outer layer introduces significant artifacts. As shown in Figure 3, the ONIOM energy for the crystal structure shows a monotonic increase from 0 to 15 kcal/mol, with the change in the Zn–O4 distance from 2.0 to 3.8 Å, while the ONIOM energy for the MD-generated snapshot decreases with increasing distance. It suggests that the active site has rearranged itself in the MD simulation when the Zn–O4 bond is cleaved. Further investigation shows that OE1 of Glu64 moves close to the Zn atom after the cleavage of the Zn–O4 bond due to the electrostatic attraction (Figure 4). The partial charge of Zn is +0.67 e, and the partial charge of OE1 of Glu64 is –0.82 e. The average distance between Zn and OE1 is 1.99 ± 0.09 Å, while the distance between Zn and O4 is 3.59 ± 0.27 Å in the MD simulation. So, the Glu64 OE1 acts

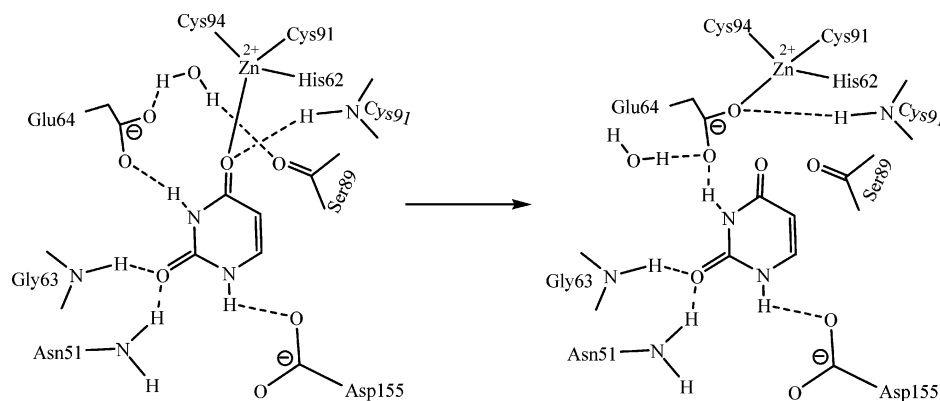


Figure 4. Rearrangement of the active site after Zn–O4 bond cleavage, as revealed by the MD simulation. Hydrogen bonds are indicated by dashed lines.

as the fourth atom coordinated with Zn after the loss of the Zn–O4 interaction. The water molecule forming a hydrogen bond with the Ser89 backbone carbonyl and the Glu64 carboxyl in the starting point moves away during the MD simulation (Figure 4). This process was not observed during the ONIOM distance scanning of the crystal structure because the backbone of Glu64 was treated as part of the outer layer and, therefore, was fixed. This restriction prohibits O4 from moving close to Zn and keeps the water molecule contained by the outer layer residues. On the other hand, during the ONIOM Zn–O4 distance scanning of the MD snapshot, the outer layer was also fixed, but it was adjusted to be suited for cleavage of the Zn–O4 bond. That is probably why the system seems to be more stable with the Zn–O4 bond cleaved in the ONIOM calculations of the MD snapshot. Therefore, the ONIOM calculations based on the crystal structure and MD snapshot may be viewed as two extremes; the crystal structure is a representation of the covalently bound Zn–O4 complex, while the MD snapshot is a representation of the unbound form of the Zn–O4 complex. One has to scan the distance between Zn and O4 and rearrange the outer layer residues at the same time to generate the energy profile correctly.

B. Combining ONIOM with MD. As discussed above, the ONIOM method with the static outer layer cannot describe the Zn–O4 bond cleavage process. MD has to be combined with ONIOM to account for the configurational changes. The scheme outlined in the Methodology section provides an approach that is computationally feasible. First, MD was used to generate snapshots with different restrained Zn–O4 distances, and then, ONIOM was used to optimize these snapshots and calculate the forces. It appears that the average of forces at individual Zn–O4 distances converges quickly, as shown in Figure 5, so only five snapshots are used for each distance, except for 2.3 Å where 10 snapshots are used. The average force decreases dramatically from 9.2 to –12.4 kcal/mol Å as the distance increases from 2.0 to 2.2 Å. Then, the force increases to –2.0 kcal/mol Å at 2.4 Å, and after that, it increase slowly to ~2 kcal/mol Å at 2.7 Å and fluctuates until 3.5 Å, where it drops to ~0 kcal/mol Å. The force curve passes zero three times; the first one is between 2.0 and 2.1 Å, indicating the first minimum in the potential of mean force curve, the second one is between 2.6 and 2.7 Å, a maximum in the potential curve, and the third one is between 3.4 and 3.5 Å, which is another minimum in the potential. The potential of mean force was calculated by using the discrete summation of the average force, as shown in Figure 6. It has a typical bond-breaking form, with one transition state for the Zn–O4 distance at approximately 2.6–2.7 Å. The barrier for the reaction is ~2.9 kcal/mol. The corresponding

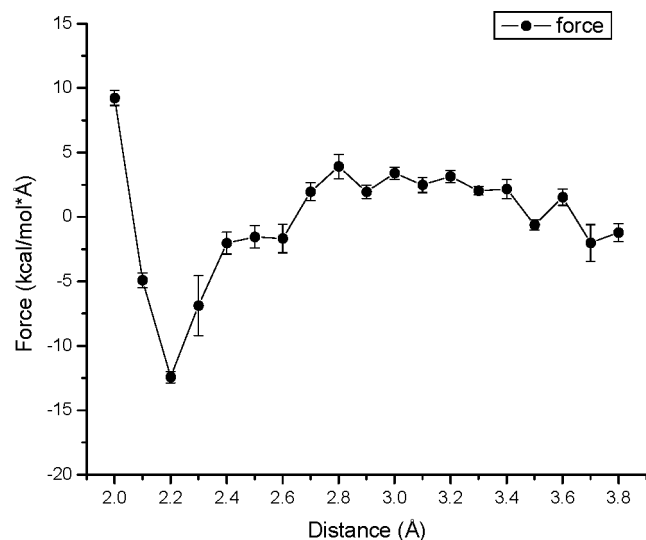


Figure 5. The average force on O4 along the Zn–O4 reaction coordinate. The bars in the plot represent the root-mean-square error from the different MD configurations at each distance.

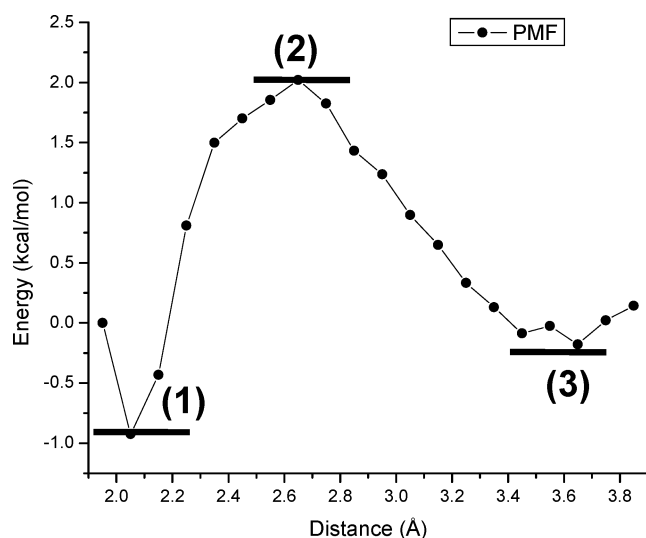


Figure 6. The potential of mean force along the Zn–O4 bond cleavage reaction coordinate.

bound, transition, and unbound states are shown in Figure 7. The transition state has the Zn pentacoordinated with His62, Cys91, Cys94, Glu64, and uracil because OE1 of Glu64 moves close to and coordinates with Zn. In fact, the bond between Zn and OE1 is formed at the beginning of the Zn–O4 bond cleavage, as shown in Figure 8. The Zn–OE1 distance decreases to 2.1 Å when the Zn–O4 distance increases to 2.4 Å. In the transition state, Zn interacts weakly with O4 of uracil since the distance is already ~ 2.6 – 2.7 Å. After the reaction, the backbone

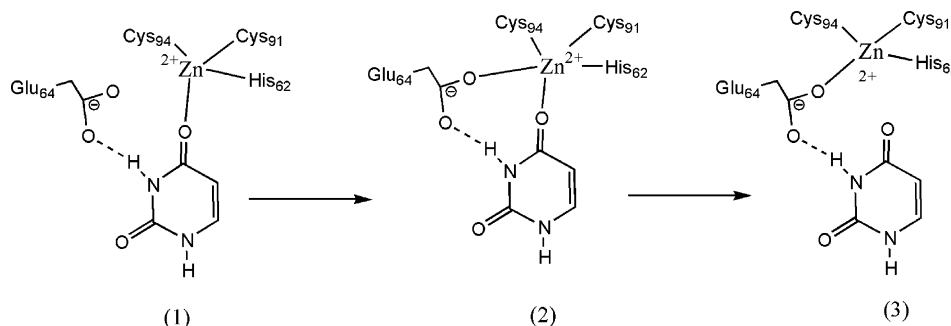


Figure 7. The bound, transition, and unbound states indicated by the PMF (see Figure 6) during the Zn–O4 bond cleavage.

amide of Cys91 forms a hydrogen bond with OE1, similar to what occurs in the MD simulation (Figure 4). Several hydrogen bond interactions between uracil and active site residues were maintained during the reaction, including Glu64 OE2 with N2H, Gly63 NH with O2, Asn55 NH2 with O2, and Asp155 OD1 with N1H, consistent with the MD simulation (Figure 4). After the Zn–O4 bond cleavage, uracil stays within the active site. It is restrained by four hydrogen bonds, including Glu64 OE2 with N2H, Gly63 NH with O2, Asn55 NH2 with O2, and Asp155 OD1 with N1H. The water molecule originally hydrogen bonded to Ser84 moves closer to Glu64 and hydrogen bonds to OE1 of Glu64.

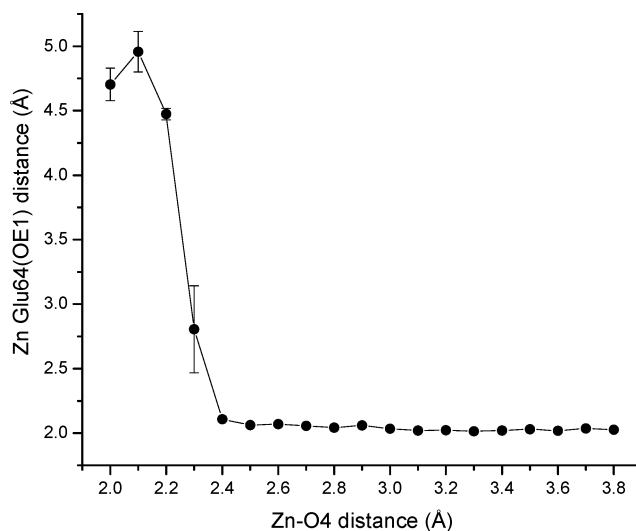


Figure 8. The distance change between Zn and Glu64 OE1 (vertical axis) during the cleavage of the Zn–O4 bond (horizontal axis).

In our calculations, Glu64 and the two Zn-ligated residues, Cys91 and Cys94, are in their anionic states, and that suggests the introduction of diffuse functions to the basis set. Therefore, the calculation was redone by using the equilibrium geometries obtained with the 6-31G** basis set and, then, by recalculating the ONIOM forces for all of the snapshots used above by adding diffuse functions with the 6-31+G** basis set. We find that the shape of the force/potential curves changes somewhat, but the conclusions are not altered. In particular, the barrier in the PMF is reduced to about 1.5 kcal/mol, indicating that the barrier remains small. (Note that, due to the limited number of force points that are practical to obtain, the integration to give the PMF also introduces some error.) Thus, we consider the agreement between the two calculations to be good.

An attempt was made to unambiguously identify the rearrangement of the outer layer during the Zn–O4 bond cleavage, but the thermal fluctuations of the atoms during the MD simulation complicate this analysis. For example, F114 in the

outer layer shows a rather large motion during the Zn–O4 bond cleavage. It also moves substantially during the MD simulation of the product complex because this residue is from a loop region. Thus, it is hard to tell whether the motion of this residue is due to the product release or not. On the other hand, Glu64 and a water molecule are easy to distinguish in this sense because both are quite stable in the active site in the product complex simulation but move significantly during the Zn–O4 bond cleavage simulation.

4. Conclusions

In this study, we revisit the Zn–O4 bond cleavage mechanism that occurs during uracil release from the active site of yCD. In the previous two-layer ONIOM calculation, we found that direct Zn–O4 bond breaking would need to overcome a huge energy barrier. Here, we first demonstrate that this barrier mainly comes from the constraint of the outer (ONIOM) layer that prohibits the proper response of active site residues to Zn–O4 bond breaking, especially the Glu64 carboxyl group. An increase of the Zn–O4 distance based on the crystal structure geometry results in a monotonic increase of energy, but the increase of the Zn–O4 distance based on the MD simulation shows a steady decrease in energy. The reason is that ONIOM optimization from the crystal structure produces a good approximation of the Zn–O4 covalently linked state, while the ONIOM optimization from a MD-based snapshot provides a better approximation of the Zn–O4 bond-broken state. The constraints imposed on the outer ONIOM layer cannot correctly describe the intermediates between the bound and a bond-broken state, which makes the ONIOM calculation always favor the starting geometry.

One strategy to address this problem is to use a QM/MM method, but the presence of Zn in the system requires a high-level QM method, which makes a straightforward combined simulation impractical. Instead, we introduced a two-step process that combines a MM classical simulation with a two-layer ONIOM QM calculation. We demonstrated that this method does describe the response of the middle layer properly. By using MD configurations that incorporate the influence of the outer layer (the remaining protein and solvent molecules) on the middle layer, conditional on the reaction coordinate value, the ONIOM-optimized energies provide a computationally realistic approach to approximate the free energy along a reaction coordinate.

In our calculations, a small number of MD snapshots (5–10) were required to obtain converged results. For the Zn–O4 bond cleavage, apparently only modest configuration changes in the reaction center region occur, leading to a relatively small number of required snapshots. In other, less favorable cases, more MD snapshots would be needed. The computational cost is dominated by the quantum calculations, indicating that a careful choice of the residue and substrate atoms to include in the inner and outer ONIOM layers and the methods to use in each layer are the key requirements for the design of a practical scheme.

The two-step approach shows that cleavage of the Zn–O4 bond occurs through a pentacoordinated Zn transition state complex. A rearrangement of some active site residues as the reaction coordinate is changed does occur. Movement of the catalytic Glu64 so that its OE1 can coordinate with the Zn takes place when the Zn–O4 distance is lengthened to ~ 2.4 Å. The electrostatic interaction between the Glu64 carboxylate and the Zn most likely provides a significant contribution to breaking the Zn–O4 bond. The barrier along this reaction coordinate is rather low, only about 2.9 kcal/mol, and therefore should not limit the rate of uracil release from the active site.

The computational result also suggests that E64 not only plays an important role in the deamination reaction as a proton shuttle but also facilitates the cleavage of the zinc–oxygen bond between the catalytic zinc and the deamination product uracil so that the product can be released. The regeneration of the enzyme requires the replacement of the zinc–OE1 coordination bond with a zinc–water coordination bond, a process that has yet to be addressed.

Acknowledgment. This work was supported by the Quantitative Biology Modeling Initiative of Michigan State University, the Michigan Center for Biological Information of the Michigan Life Sciences Corridor, and NIH grants (GM58221 to H.Y. and GM47274 to R.I.C.).

References and Notes

- (1) Yao, L. S.; Li, Y.; Wu, Y.; Liu, A. Z.; Yan, H. G. *Biochemistry* **2005**, *44*, 5940.
- (2) Sklenak, S.; Yao, L. S.; Cukier, R. I.; Yan, H. G. *J. Am. Chem. Soc.* **2004**, *126*, 14879.
- (3) Vreven, T.; Mennucci, B.; da Silva, C. O.; Morokuma, K.; Tomasi, J. *J. Chem. Phys.* **2001**, *115*, 62.
- (4) Vreven, T.; Morokuma, K.; Farkas, O.; Schlegel, H. B.; Frisch, M. J. *J. Comput. Chem.* **2003**, *24*, 760.
- (5) Svensson, M.; Humbel, S.; Froese, R. D. J.; Matsubara, T.; Sieber, S.; Morokuma, K. *J. Phys. Chem.* **1996**, *100*, 19357.
- (6) Maseras, F.; Morokuma, K. *J. Comput. Chem.* **1995**, *16*, 1170.
- (7) Dudev, T.; Lim, C. J. *J. Phys. Chem. B* **2001**, *105*, 10709.
- (8) Singh, U. C.; Kollman, P. A. *J. Comput. Chem.* **1986**, *7*, 718.
- (9) Field, M. J.; Bash, P. A.; Karplus, M. *J. Comput. Chem.* **1990**, *11*, 700.
- (10) Warshel, A. *Computer Modeling of Chemical Reactions in Enzymes*; Wiley: New York, 1991.
- (11) Aqvist, J.; Warshel, A. *Chem. Rev.* **1993**, *93*, 2523.
- (12) Stanton, R. V.; Hartsough, D. S.; Merz, K. M. *J. Phys. Chem.* **1993**, *97*, 11868.
- (13) Gao, J. *Acc. Chem. Res.* **1996**, *29*, 298.
- (14) Gao, J., Ed. *Methods and Applications of Combined Quantum Mechanical and Molecular Mechanical Potentials*; VCH: New York, 1996; Vol. 7, p 119.
- (15) Friesner, R. A.; Beachy, M. D. *Curr. Opin. Struct. Biol.* **1998**, *8*, 257.
- (16) Cui, Q.; Guo, H.; Karplus, M. *J. Chem. Phys.* **2002**, *117*, 5617.
- (17) Gao, J. L.; Truhlar, D. G. *Annu. Rev. Phys. Chem.* **2002**, *53*, 467.
- (18) Cui, Q.; Karplus, M. *Adv. Protein Chem.* **2003**, *66*, 315.
- (19) Elstner, M.; Frauenheim, T.; Suhai, S. *J. Mol. Struct.: THEOCHEM* **2003**, *632*, 29.
- (20) Li, G. H.; Zhang, X. D.; Cui, Q. *J. Phys. Chem. B* **2003**, *107*, 8643.
- (21) Pu, J. Z.; Gao, J. L.; Truhlar, D. G. *J. Phys. Chem. A* **2004**, *108*, 5454.
- (22) Hu, H.; Yang, W. T. *J. Chem. Phys.* **2005**, *123*, 041102.
- (23) Konig, P. H.; Hoffmann, M.; Frauenheim, T.; Cui, Q. *J. Phys. Chem. B* **2005**, *109*, 9082.
- (24) Kuno, M.; Hannongbua, S.; Morokuma, K. *Chem. Phys. Lett.* **2003**, *380*, 456.
- (25) Sousa, S. F.; Fernandes, P. A.; Ramos, M. J. *J. Mol. Struct.: THEOCHEM* **2005**, *729*, 125.
- (26) Cerqueira, N.; Fernandes, P. A.; Eriksson, L. A.; Ramos, M. J. *Biophys. J.* **2006**, *90*, 2109.
- (27) Zhan, C. G.; Gao, D. Q. *Biophys. J.* **2005**, *89*, 3863.
- (28) Yang, W.; Drueckhammer, D. G. *J. Phys. Chem. B* **2003**, *107*, 5986.
- (29) Zhang, Y. K.; Liu, H. Y.; Yang, W. T. *J. Chem. Phys.* **2000**, *112*, 3483.
- (30) Yao, L. S.; Sklenak, S.; Yan, H. G.; Cukier, R. I. *J. Phys. Chem. B* **2005**, *109*, 7500.
- (31) Pearlman, D. A.; Case, D. A.; Caldwell, J. W.; Ross, W. S.; Cheatham, T. E.; Debolt, S.; Ferguson, D.; Seibel, G.; Kollman, P. *Comput. Phys. Commun.* **1995**, *91*, 1.
- (32) Frisch, M. J.; Trucks, G. W.; Schlegel, H. B.; Scuseria, G. E.; Robb, M. A.; Cheeseman, J. R.; Montgomery, J. A., Jr.; Vreven, T.; Kudin, K. N.; Burant, J. C.; Millam, J. M.; Iyengar, S. S.; Tomasi, J.; Barone, V.; Mennucci, B.; Cossi, M.; Scalmani, G.; Rega, N.; Petersson, G. A.; Nakatsuji, H.; Hada, M.; Ehara, M.; Toyota, K.; Fukuda, R.; Hasegawa, J.; Ishida, M.; Nakajima, T.; Honda, Y.; Kitao, O.; Nakail, H.; Klene, M.; Li, X.; Knox, J. E.; Hratchian, H. P.; Cross, J. B.; Bakken, V.; Adamo, C.; Jaramillo, J.; Gomperts, R.; Stratmann, R. E.; O. Yazyev, A. J. A.; Cammi, R.; Pomelli, C.; Ochterski, J. W.; Ayala, P. Y.; Morokuma, K.; Voth, G. A.; Salvador, P.; Dannenberg, J. J.; Zakrzewski, V. G.; Dapprich, S.; Daniels,

A. D.; Strain, M. C.; Farkas, O.; Malick, D. K.; Rabuck, A. D.; Raghavachari, K.; Foresman, J. B.; Ortiz, J. V.; Cui, Q.; Baboul, A. G.; Clifford, S.; Cioslowski, J.; Stefanov, B. B.; G. Liu, A. L.; Piskorz, P.; Komaromi, I.; Martin, R. L.; Fox, D. J.; Keith, T.; Al-Laham, M. A.; Peng, C. Y.; Nanayakkara, A.; Challacombe, M.; Gill, P. M. W.; Johnson, B.; Chen, W.; Wong, M. W.; Gonzalez, C.; Pople, J. A. *Gaussian 03*, revision C.02; Gaussian, Inc.: Wallingford, CT, 2004.

(33) Becke, A. D. *J. Chem. Phys.* **1993**, *98*, 5648.

(34) Ireton, G. C.; Black, M. E.; Stoddard, B. L. *Structure* **2003**, *11*, 961.

(35) Carlow, D. C.; Smith, A. A.; Yang, C. C.; Short, S. A.; Wolfenden, R. *Biochemistry* **1995**, *34*, 4220.

(36) Carlow, D. C.; Short, S. A.; Wolfenden, R. *Biochemistry* **1996**, *35*, 948.

(37) Ko, T. P.; Lin, J. J.; Hu, C. Y.; Hsu, Y. H.; Wang, A. H. J.; Liaw, S. H. *J. Biol. Chem.* **2003**, *278*, 19111.